

Numerical investigation of non-Newtonian fluid flow in channels with local expansion

Amir haghghatkah *, Milad abdollahi kahriz.

1. Master of Mechanical Engineering,
Doctor of Mechanical Engineering,

Abstract

Fluids can be classified from different perspectives. From the perspective of fluid behavior under the influence of shear stress, the fluids can be classified into Newtonian and non-Newtonian fluids. Newtonian fluid is a material in which shear stress without yield stress (at zero shear rate is zero shear stress) is only a linear function of shear rate and in this material shear stress to shear rate is called viscosity. In non-Newtonian fluids one of the two Newtonian fluid conditions (zero yield stress condition or shear stress linearity condition in terms of shear rate) or both conditions are not met simultaneously. In other words, it can be said that a non-Newtonian fluid is a fluid in which either the shear stress diagram is nonlinear in shear rate or if the diagram is linear it does not cross the origin of the coordinates.

In this study, the study of non-Newtonian fluid flow in a rectangular cross-section channel for sudden discontinuity is investigated. The expansion coefficient is assumed to be 3 and the fluid flow is investigated in two-dimensional steady state. For numerical simulation, Poly flow commercial software, which is a subset of Ennis software, is used specifically to simulate non-Newtonian fluids. For different Reynolds, Weissenberg and Beta numbers, the vortex length has been measured in different conditions and the influence of the mentioned parameters on the vortex length has been investigated. Finally, contours of the flow lines are presented to determine the vortex length using them. It should be noted that the non-Newtonian fluid discussed in this study was selected from the type of oldroyd B fluid.

Keywords: Local Expansion, Non-Newtonian Fluid, Numerical Simulation, Poly flow Software.

Date of Submission: 16-11-2020

Date of Acceptance: 02-12-2020

I. Introduction

Non-Newtonian fluid mechanics has been the subject of much interest by researchers since the late 19th century. And in those years the basic theories of this science were built. Among non-Newtonian fluids, viscoelastic fluids have received much attention due to their many applications and have been the subject of much research. Non-Newtonian fluids are widely used in military, medical, and industrial activities, which have long been the focus of attention. The science of studying non-Newtonian fluid flow has become known as rheology today, and because of the specific properties of such fluids, different and unexpected behaviors of such fluids occur. The purpose of this study was to investigate the viscoelastic fluid flow and its heat transfer in pipes with local expansion, mathematical modeling, its solution and then analyzing and evaluating the existing solution.

Fluid flow is particularly important in plate divergent transforms. These transformations have relatively simple geometries and relatively complex flow patterns.

In examining Newtonian fluid flow within the geometry of sudden expansion, preliminary research has been conducted in the form of experimental work by Durst et al. [1], Cherdron et al. [2] and Ouwa et al. [3]. By examining the flow downstream of the symmetric two-dimensional sudden expansion, they showed that for low Reynolds numbers, the flow remained symmetric, but for larger Reynolds numbers, asymmetric conditions for the vortices created rotational zones of different sizes. When the flow in the symmetric divergent plate transforms loses its symmetry, it produces vortices of different lengths. Such a phenomenon that results in the production of asymmetric vortices is called Bifurcation Phenomena. If the vortex length is plotted in terms of Reynolds, this phenomenon is clearly visible.

Numerical study of the flow for 3: 1 expansion ratio by Fearn et al. [4] and Durst et al. [5] has resulted in finding a critical Reynolds number for the flow transfer from symmetric to asymmetric state and also plotted diagram. Numerical investigation of the relative impact of expansion on the vortex bifurcation phenomenon for Newtonian fluid has been carried out by Battaglia et al. [6] and Allerborn et al. They observed stability

improvement by using symmetric resolution in their studies by reducing the expansion ratio. The study of bifurcation phenomena for sudden plate expansion flow at larger expansion ratios was studied by Revuelta [8].

Also in their study, Abbott and Kline[9] investigated asymmetric turbulent flows through symmetric plate-plane ducts. The instability structure of the multi-branch phenomenon has also been studied by Mizushima and Shiotani [10] using nonlinear analysis.

Oliveira[11], Ternik et al. [12], using numerical simulation, obtained a critical Reynolds number based on upstream altitude and mean channel inlet velocity of 54. Using a quadratic finite difference method in the investigation of sudden divergent intra-channel flow with a 3: 1 expansion ratio in Drake's study, a critical Reynolds number of 53.3 is reported. Hawa and Rusak[14] reported a critical Reynolds number of 53.8 using the linear stability analysis method and the finite difference method on the flow function and the vortices function for a 3: 1 sudden expansion ratio. And in this geometry Mishra and Jayaraman[15] have obtained a critical Reynolds value in their research by applying the finite element method and Continuation–Perturbation method.

The range of Reynolds numbers and divergence ratios is broader in the study by Dagtekin and Unsal [16] in the field of Newtonian fluids for divergence. In this study, Reynolds ranges from 0.1 to 500 and the divergence ratio is in the range of 1.5 to 500. In this research, the vortices have been investigated in both plane and axial symmetry states. Scott and Mirza [17] also examined in their research the Newtonian fluid flow in plate divergence. By solving the two-dimensional Navier-Stokes equations using finite element method, they show that the vortices change linearly with Reynolds in plate divergent conversion.

Oliveira et al. [18] obtained the eddy length and pressure drop coefficient in various states by numerically solving the Newtonian fluid flow in a symmetric plate-plane divergence for the expansion ratios of 1.5 to 4 and in the range of 0.5 to 200 Reynolds. As can be seen from their research, the vortex length has a direct relationship with the Reynolds number, and at all divergence ratios, the vortex length increases with increasing Reynolds number. At low Reynolds numbers, increasing the conversion ratio decreases the vortex length, and at high Reynolds numbers, increasing the conversion ratio increases the vortex length. Also Schreck and Schafe [19] studied the flow field in sudden expansion using the finite volume method and investigated the influence of different expansion rates on the vortex length.

Shapira et al. [20] investigated the phenomenon occurring along the vortex by analyzing the linear stability for the symmetric flow in a sudden plate expansion. Durst et al. [21] also investigated the empirical and numerical study of the sudden expansion with a 1: 2 expansion ratio, the vortex length and their length difference. In their research Fletcher et al. [22] studied the effect of the type of input velocity profile on the flow parameters by examining the flow in the symmetric sudden expansion.

Pinho et al. [23] also showed in their investigations of sudden plate expansion currents that for low Reynolds numbers, the velocity distribution at the expansion section level slightly detracts from its parabolic profile. Hawa and Rusak[24] studied the effect of channel geometry asymmetry on the behavior of these currents.

In recent decades, asymmetric flow of non-Newtonian fluids in symmetrical plate divergence has been the focus of many researchers. The purpose of most research in this area is to find the critical Reynolds number at different divergence ratios and to investigate the vortex length. In non-Newtonian fluid flow, the flow changes that result in changes in the intensity and size of the bridges are also dependent on the non-Newtonian fluid properties in addition to the Reynolds number. For this reason, most of the studies use either the generalized Reynolds number or the modified Reynolds number, which incorporates non-Newtonian fluid properties. Bell and Surana [25] studied the flow of non-Newtonian fluid at an asymmetric sudden expansion with a 1: 2 expansion ratio. In their research using the power law model, for Reynolds number 10, they investigated the dependence of vortex size and length on the index value. Ternik [26] investigated the effects of non-Newtonian properties on the transition from symmetric to asymmetric flow in the sudden divergence ratio of 1: 3. His model, power dilution fluid, and power index and Reynolds range are considered in the range of 0.6 to 1 and 10 to 150, respectively. Ternik's results [26] show that fluid dilution behavior (reduction of power index) on one hand reduces the flow pressure drop in divergent transformations and on the other hand increases the critical generalized Reynolds number. In other words, the fluid dilution behavior causes the flow to be asymmetric at higher speeds. In his research, he presented a diagram that clearly shows the dilution of fluid pressure. Manica et al. [27], using the finite difference numerical method, investigated the non-Newtonian fluid flow with a power model ($0 < n < 2$) to convert a sudden divergence to a 1: 3 expansion ratio and n each power index. Reynolds has reported a crisis. Due to the range of power indices n in this study, both dilution and thickening behavior have been investigated and the results show that dilution behavior ($n < 1$) delayed the phenomenon of bifurcation and for concentrated state Humidity is the result of the opposite. Neofytou [28] reported the critical Reynolds number values 33 and 44 by numerical analysis of the non-Newtonian fluid flow for the power model and the quadratic model, respectively. His results also show that the extension length and pressure drop are greater for the concentrated fluid than for the Newtonian fluid. Ternik et al [29] studied non-

Newtonian fluid flow with these two models and reported a critical Reynolds number and plotted a multilevel diagram for studying the vortex length. Paket al.[30] investigated empirically the effect of non-Newtonian and viscoelastic properties on vortex lengths at conversion ratios of 2 and 2.667 by empirically investigating viscoelastic fluid flow in axial symmetric divergent conversion. The results show that for laminar flow regime, the vortex length in viscoelastic fluid is less than Newtonian fluid and in turbulent flow regime, the viscoelastic fluid vortex length is several times more than Newtonian fluid. The Reynolds number is also defined as the generalized Reynolds number in the study to include the power index n . Norouzi et al. [31] investigated the laminar and incompressible flow of viscoelastic fluid in two-dimensional plate divergence with gradual expansion at 30, 45, 60, and 90 ° expansion angles and 1: 3 expansion ratio. They studied the symmetric and asymmetric vortex lengths over a wide range of Reynolds and Weissenberg numbers using a nonlinear Fine-Tanner model to simulate viscoelastic fluid stress terms. Cruz et al. [32] calculated the Nusselt number and non-Newtonian fluid friction coefficients in direct channels using the generalized Newton, Carreau-Yasuda, HerschelBulkley, Bingham and linear form PTT models. Jalali et al. [33] numerically simulated the developed and non-isothermal viscoelastic fluid flow inside the medial canal using a simplified PTT rheological model. They calculated the temperature distribution and the Nusselt number for values of $-10 \leq Br \leq 10$, assuming the properties of the viscoelastic fluid to be temperature dependent. The results presented by them show that the Nusselt number decreases with increasing Br content. Baptista et al. [34] numerically simulated the non-Newtonian fluid flow between two parallel plates and inside the tube using a power model and a constant temperature boundary condition and calculated the Nusselt number for different values of the power law. Alves et al. [35] investigated the flow of Newtonian and viscoelastic fluid inside a tube with constant and uniform boundary conditions using the method used by Cruz et al[32]. Norouzi [36] developed an analytical solution for the heat transfer of viscoelastic fluid inside the axial tube using the PTT rheological model and calculated the Nusselt temperature and number at different positions. Letelier et al [37] used the generalized PTT model to analytically simulate the Graetzproblem for direct-channel viscoelastic fluid. They studied secondary stream formation, temperature and Nusselt number. Shahbani-Zahiri et al. [38] numerically simulated the heated and cooled viscoelastic flow within a two-dimensional channel with sudden expansion. They addressed the impact of tennis on overall casualties.

II. Governing equations

The general equation governing the flow of a fluid of type oldroyd B can be illustrated as follows:

$$\rho \frac{dV}{dt} = -\nabla P + \text{div}S + J \times B + r \quad (1)$$

$$\text{div}V = 0 \quad (2)$$

In the above relation $V = (u, v, w)$ denotes velocity field and ρ denotes fluid density and P represents hydrostatic pressure. r is also known as Darcy's resistance to OL fluid, and S represents the additional stress tensor defined for OL fluid as follows [13]:

$$\left(1 + \lambda^\alpha \frac{D^\alpha}{Dt^\alpha}\right) S = \mu(1 + \theta^\beta \frac{D^\beta}{Dt^\beta}) A_1 \quad (3)$$

In the above relation μ expresses the dynamic viscosity of fluid, λ denotes rest time and θ denotes delay time. Also α and β are computational parameters such that $0 \leq \alpha \leq \beta \leq 1$. The A_1 , also known as the first Rivlin-Ericksen tensor, is defined as follows:

$$A_1 = \nabla V + (\nabla V)^T \quad (4)$$

In the above relation ∇ it represents the gradient operator and T represents the inverse of the matrix. We also have:

$$\frac{D^\alpha S}{Dt^\alpha} = \frac{\bar{D}^\alpha S}{Dt^\alpha} + (V \cdot \nabla)S - S(\nabla V)^T \quad (5)$$

$$\frac{\bar{D}^\alpha f(t)}{Dt^\alpha} = \frac{1}{\Gamma(1-\alpha)} \frac{d}{dt} \int_0^T (t-\xi)^{-\alpha} f(\xi) d\xi, \quad 0 < \alpha < 1 \quad (6)$$

In the above relation Γ is the expression of the gamma function. When $\alpha = \beta = 1$, equation (3) denotes the equation governing the first-order oldroyd B fluid. If we put $\lambda = \theta = 0$ in the first order oldroyd B relation, we arrive at the same classical Navier-Stokes equations.

The Maxwell equation can also be written as follows:

$$\text{div}B = 0, \text{curl}B = \mu_m J, \text{curl}E = -\frac{\partial B}{\partial t} \quad (7)$$

In the above relation J is the instantaneous density and B represents the magnitude of the magnetic fluxes into the fluid stream as shown below:

$$B = B_0 + b \quad (8)$$

In relation (8), B_0 and b represent the magnetic field applied and created by the flow of fluid, respectively.

Also μ_m represents the magnetic permeability and finally E represents the electric field. It should be noted that no voltage is applied to the cysteine and no dipole event occurs so $E = 0$ can be omitted b . The effect of Hall's phenomenon can also be seen as follows:

$$\mathbf{J} \times \frac{w_e t_e}{B_0} (\mathbf{J} \times \mathbf{B}) = \sigma [\mathbf{E} + \mathbf{V} \times \mathbf{B} \times \frac{1}{en_e} \nabla P_e] \quad (9)$$

In the above relation w_e is the cyclotron frequency of the electrons and t_e is the collision time of the electrons. σ is the electrical conductivity, e is the electric charge, n_e the electron density and P_e the electron pressure. It should be noted that no thermoelectric and ion slip effects have been observed in this respect [12].

The two most important parameters that will be used in this research are the Weissenberg number and the beta number. In fact, the Weissenberg number is defined as the ratio of the force of an elastic property to the force of a fluid viscosity that can be mathematically written as follows:

$$Wi = \lambda \dot{\gamma} \quad (10)$$

In the above relation λ the material characteristic time (time of stress relief) and $\dot{\gamma}$ are the shear rate of flow. The relaxation time for the stress is very small for Newtonian fluids (less than 10^{-6} to 10^{-4} seconds) and for large numerical elastic solids (greater than 100 seconds). The smaller the Weissenberg number for a material, the more likely it is that it will flow. When the Weissenberg number is zero, the fluid behaves similar to the Newtonian fluid behavior.

The beta number can also be defined as follows:

$$\beta = \frac{\eta_{mo}}{\eta_0} \quad (11)$$

In the above relation η_{mo} the viscosity of the soluble material is at zero shear rate. Also η_0 is total viscosity of the solution at zero refraction rate is calculated as follows:

$$\eta_0 = \eta_N + \eta_{mo} \quad (12)$$

In the above relation, η_N represents the solvent viscosity.

III. Problem assumptions

In the present study, the problem geometry is considered as two-dimensional and incompressible fluid flow. The range of Reynolds numbers used in the present study for the laminar flow regime is briefly summarized as the main assumptions considered in this study.

1. The flow is two-dimensional and smooth.
2. The viscoelastic fluid is incompressible.
3. A constant temperature is assumed so that the current is not temperature dependent.
4. Reynolds is considered to be within the range of a slow flow regime.
5. The effects of gravitational acceleration and volume forces have been avoided.

IV. Geometry of the problem

The problem geometry consists of two channels with a square cross-section that are in contact with each other. The side length of the channel cross-sectional area is considered to be smaller and the length of the cross-sectional area of the channel is considered to be larger. A schematic view of the channel being considered in this project with its dimensions can be seen in Figure (1).

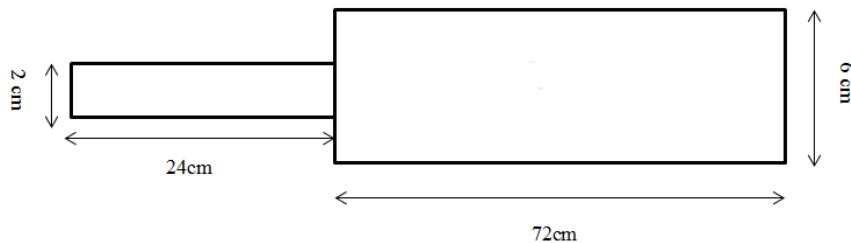


figure 1. Schematic view of the investigated channel

V. Boundary conditions

The channel input will use the input speed boundary condition. We know that the channel input can be considered as a uniform input speed. At the outlet of the channel, since the fluid is assumed to be discharged into the environment, then the use of the outlet boundary condition is a reasonable and accurate pressure. It should be noted that in this case the output pressure gauge is zero. In the case of canal walls, the term non-slip fluid on the wall should also be used, which assumes that the velocity of the fluid on the wall is equal to the velocity of the wall, and in this case, since the channel wall is constant, it can be said that the fluid velocity on the wall is Channel will be zero.

The problem solving algorithm in poly flow software is illustrated in Figure (2).

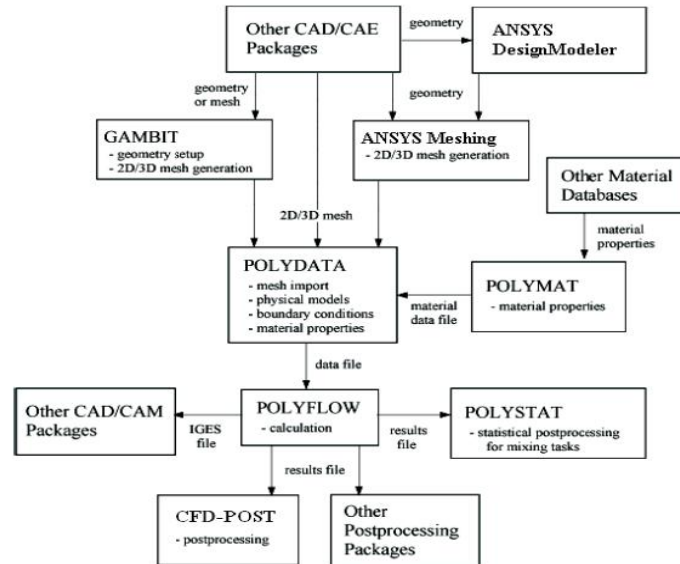


figure 2. General problem-solving structure with PolyFlow software

VI. Solution independence from mesh

To ensure the independence of the solution from the mesh and to ensure that the meshes are sufficiently selected and smaller, and to reduce the size of most meshes, despite the increased computational costs, they do not have a significant effect on the output response, the vortex lengths formed for the three Different types of patches will be examined. Table 1 shows the number of elements considered in each case along the length of the formed vortices. The percentage of relative error is also calculated.

Table 1. Examine the number of elements and the length of the vortex and relative error for different milling states

Case	Number of elements	vortex length	relative percentage error
1	48000	4.94	1.2%
2	108000	4.9	0.4%
3	432000	4.88	-

As shown in Table (1), by increasing more than four-fold the elements from the second state to the third state, only 0.4% of the vortex length changes, which is a very small amount. Therefore, the latter is regarded as the basic one.

Next, we will calculate the vortex lengths for the different modes of beta, Weissenberg and Reynolds and arrange them in a table. It should be noted that throughout the calculations we will consider the total density constant and equal to 750 Kg / s as well as the total viscosity constant and equal to 0.01.

VII. Results

In the first case, we consider beta equal to 0.1 and Reynolds number 1, and we calculate the vortex length for 5 different Weissenberg numbers, which are presented in Table (2). The velocity contours of these modes are also shown in Figures (3), respectively.

Table 2. Vortex lengths per beta equal to 0.1, Reynolds equals 1, and different Weissenberg

No.	Weissenberg	vortex length
1	0.05	1.45
2	0.1	0.9
3	0.15	0.75
4	0.2	0.56
5	0.25	0.34

At very small Weissenberg numbers, the Newtonian fluid exhibits behavior, so the velocity contour at small Weissenberg numbers is very similar to the Newtonian fluid velocity contour. But for large Weissenberg numbers the condition of expansion is established, and the larger the Weissenberg number, the fluid flow takes longer to reach the condition of expansion. As the Weissenberg number increases, the first and second

critical Reynolds number also decreases. As a result, the vortex length also decreases with increasing Weissenberg numbers.

In the latter case the beta equals 0.1 and the Reynolds number is 100 and is calculated for the 5 different Weissenberg numbers shown in table (3).

Table 3. Beta vortex lengths equal to 0.1, Reynolds equals 100, and different Weissenberg

No.	Weissenberg	vortex length
1	0.05	3.91
2	0.005	5.50
3	0.0005	5.54
4	0.00005	5.56
5	0.000005	5.57

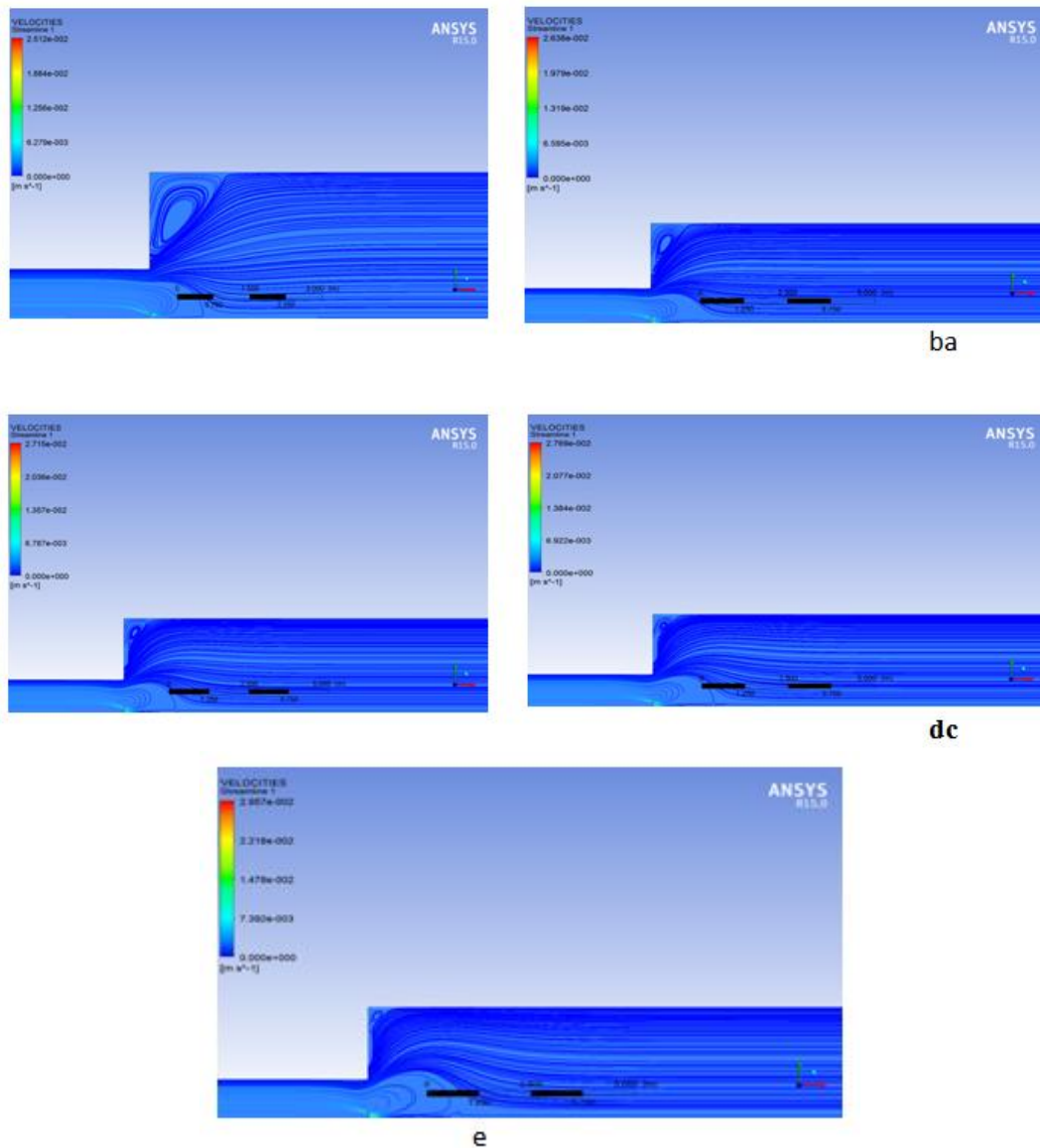


Figure 3. Vortex length per Reynolds one and a. Beta equal to 0.1 and Weissenberg equal to 0.05 b. Beta for 0.1 and Weissenberg for 0.1 c. Beta equal to 0.1 and Weissenberg 0.15 d. The beta is 0.1 and the Weissenbergs 0.2. Beta equals 0.1 and Weissenbergequals 0.25

In the third case the beta is 0.9 and the Reynolds number is 100 and the vortex length is calculated for 5 different Weissenberg numbers as shown in Table (4).

Table 4. Vortex lengths per beta equal to 0.9 and Reynolds equals 100 and different Weissenberg

No.	Weissenberg	vortex length
1	5	5.43
2	2	5.5
3	0.2	5.54
4	0.5	5.56
5	0.005	5.57

The fourth beta is 0.9 and the Reynolds number is 1 and is calculated for 5 different Weissenberg vortex lengths as shown in Table 5.

Table 5. Vortex lengths per beta equal to 0.9 and Reynolds equals 1 and different Weissenberg

No.	Weissenberg	vortex length
1	0.005	2.43
2	2.5	2.9
3	5	2.34
4	7.5	2.28
5	10	1.44

In the fifth case, Weissenberg equals 0.5 and Reynolds number 1, and is calculated for 5 different beta vortex lengths as shown in Table 6.

Table 6. Vortex lengths for Weissenberg equals 0.5 and Reynolds equals 1 and different beta

No.	Beta number	vortex length
1	0.1	0.34
2	0.3	0.8
3	0.5	1.5
4	0.7	2.1
5	0.9	2.39

In the sixth case, Weissenberg equals 0.005 and Reynolds number 1, and is calculated for 5 different beta vortex lengths, which are presented in Table 7.

Table 7. Vortices for Weissenberg equals 0.005 and Reynolds equals 1 and different beta

No.	Beta number	vortex length
1	0.1	2.34
2	0.3	2.41
3	0.5	2.44
4	0.7	2.45
5	0.9	2.47

In the seventh case, Weissenberg equals 0.05 and Reynolds number 100, and is calculated for 5 different beta vortex lengths as shown in Table (8).

Table 8. Weissenberg vortex lengths 0.05 Reynolds equals 100 and different beta

No.	Beta number	vortex length
1	0.1	3.93
2	0.3	4.91
3	0.5	5.12
4	0.7	5.31
5	0.9	5.56

As can be seen, the length of the gaps has increased with increasing beta.

In the eighth state, Weissenberg equals 0.0005 and Reynolds number 100, and is calculated for 5 different beta vortex lengths as shown in Table 9.

Table 9. Vortices for Weissenberg equals 0.0005 and Reynolds equals 100 and different beta

No.	Beta number	vortex length
1	0.1	5.5
2	0.3	5.57
3	0.5	5.58
4	0.7	5.59
5	0.9	5.6

As can be seen, the length of the gaps has increased with increasing beta. In the eighth state, Weissenberg equals 0.0005 and Reynolds number 100, and is calculated for 5 different beta vortex lengths as shown in Table 9.

Table 9. Vortices for Weissenberg equals 0.0005 and Reynolds equals 100 and different beta

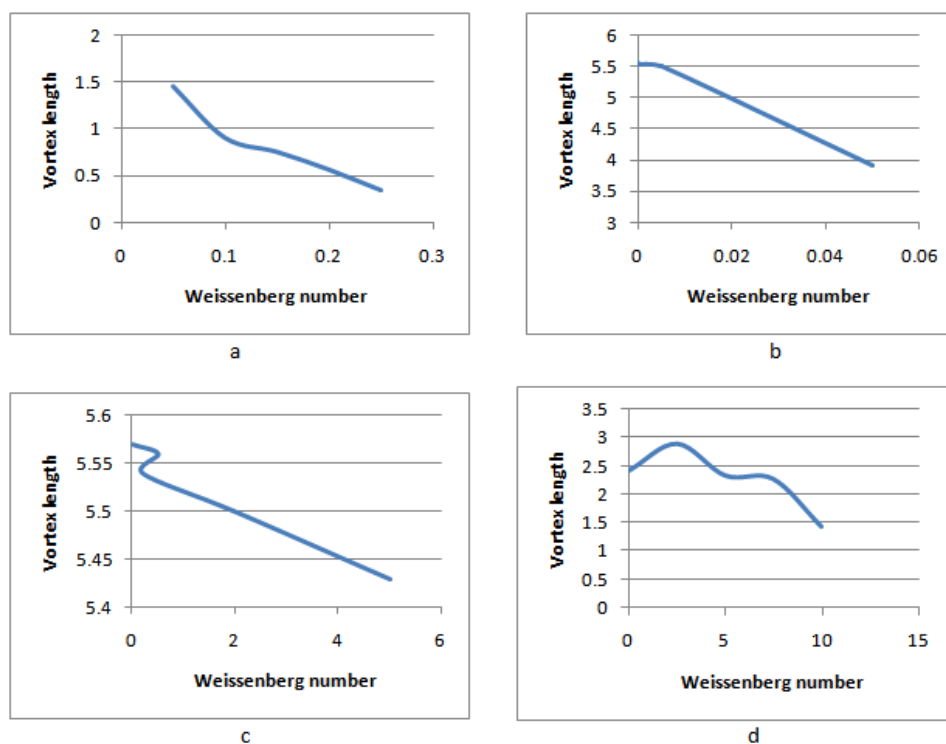
No.	Beta number	vortex length
1	0.1	5.5
2	0.3	5.57
3	0.5	5.58
4	0.7	5.59
5	0.9	5.6

In Weissenberg's ninth case, the beta is 0.005 and the beta is 0.1, and the vortex length is calculated for 6 different Reynolds numbers given in Table 10.

Table 10. Vortex lengths for Weissenberg equals 0.005 and beta equals 0.1 and different Reynolds

No.	Reynolds number	vortex length
1	100	5.5
2	80	5.36
3	60	5.1
4	40	4.9
5	20	4.5

In Fig. 4, the vortex length is plotted in different conditions.



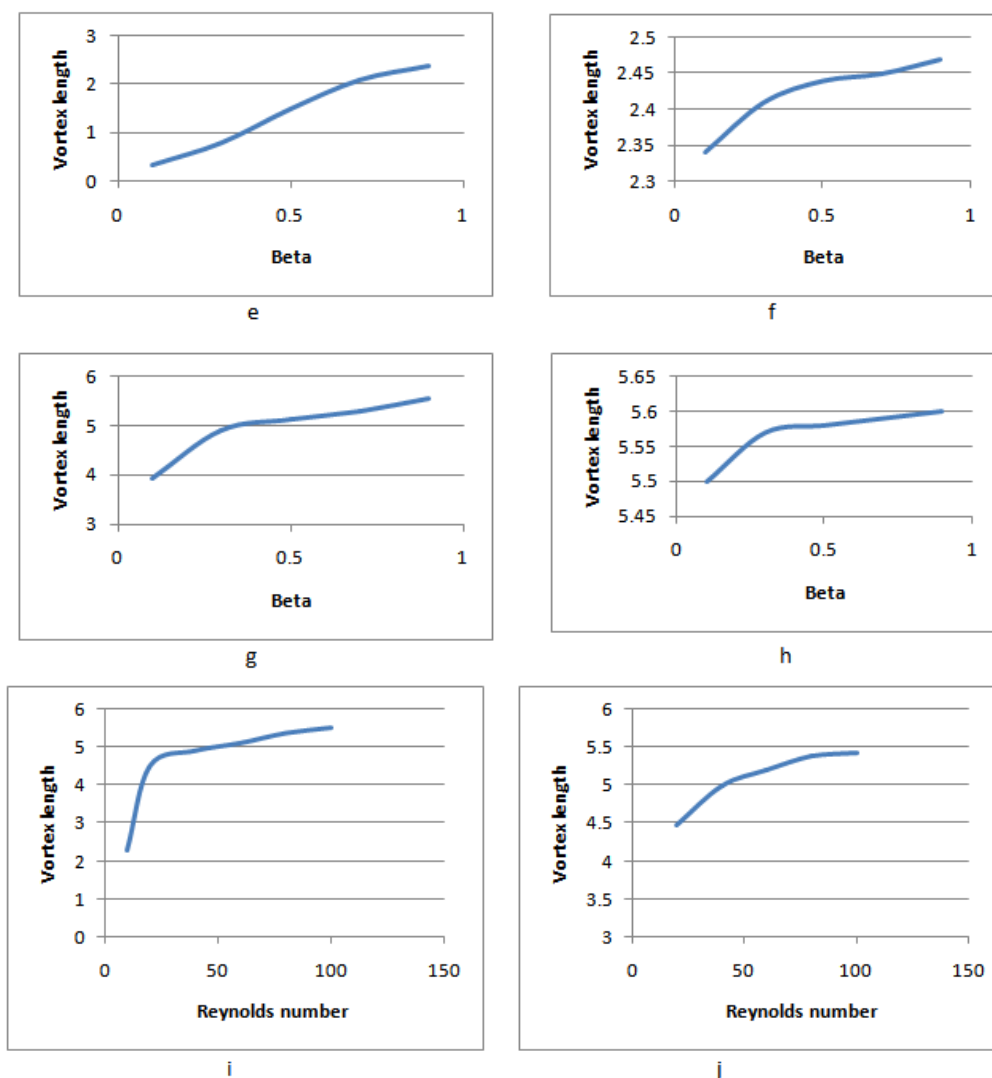


Figure 4. Vortex lengths per a. Beta equal to 0.1 and Reynolds equal to 1 and different Weissenberg. b. Beta equal to 0.1 and Reynolds equal to 100 and Weissenberg different. c. Beta equal to 0.9 and Reynolds equal to 100 and Weissenberg. d. Beta equals 0.9 and Reynolds equals 1 and Weissenberg. e. Weissenberg equals 0.5 and Reynolds equals 1 and different beta. f. Weissenberg equals 0.005 and Reynolds equals 1 and different beta. g. Weissenberg equals 0.05 Reynolds equals 100 and different beta. h. Weissenberg equals 0.0005 and Reynolds equals 100 and different beta. i. Weissenberg equals 0.005 and beta equals 0.1 and different Reynolds. j. Weissenberg equals 5 and beta of 0.9 and various Reynolds

VIII. Conclusion

By comparing the vortex length when Reynolds number is set to 100 and Reynolds number is set to 1, we can conclude that in both cases the beta number is constant. The vortex length also increases with increasing Reynolds number. In fact, as the Reynolds number increases, the inlet velocity increases and some of this kinetic energy must be depreciated after a sudden expansion. As the energy dissipation occurs by the vortices formed, the vortices have to be longer in order to depreciate more energy. By increasing the beta number, the fluid properties completely deviate from the Newtonian fluid state and favor the behavior of non-Newtonian fluids. As can be seen, the vortex length does not change with the increase of the beta number and thus the viscosity. Because viscosity does not affect the amount of turbulence.

In the sound with the beta constant and the Reynolds number constant, with the increase of the Weissenberg number, the vortex length decreases with increasing shear stress. As the shear stress increases, the kinetic energy loss increases and the kinetic energy decreases during the vortex.

When the Weissenberg and Reynolds number is constant and the beta is increased because the fluid behavior becomes more non-Newtonian and the viscosity also increases, the vortex length increases.

For the case of Weissenberg 0.005, the vortex length for different beta was increased by increasing beta, while for Weissenberg was 0.005, the vortex length was increased to 0.005. The different beta is almost the same.

Compared to the seventh and eighth states, when Reynolds was 100 and Weissenberg was 0.05, the wavelengths of the wavelets in different beta were reduced by decreasing the Weissenberg number to 0.0005, but the wavelengths in the lower beta were more pronounced but slightly smaller. There are differences.

Therefore, it can be briefly stated that in non-Newtonian fluid flow, the vortex length is directly related to the Reynolds number and increases with the Reynolds number. The vortex length also increases with increasing beta. But the vortex length is inversely proportional to the Weissenberg number, with the Weissenberg number decreasing as the vortex length decreases, which is more pronounced at high Reynolds numbers. At very small Weissenberg numbers the fluid behavior is Newtonian.

Reference

- [1]. Durst F., Melling A., Whitelaw J. H., (1974), "Low Reynolds number flow over a plane symmetric sudden expansion", *J. Fluid Mechanics*, Vol. 64, pp. 111–128.
- [2]. Cherdron W., Durst F., Whitelaw J. H., (1978), "Asymmetric flows and instabilities in symmetric ducts with sudden expansions", *J. Fluid Mechanics*, Vol. 84, pp. 13–31.
- [3]. Ouwa Y., Watanabe M., Asawo H., (1981), "Flow visualization of a two-dimensional water jet in a rectangular channel", *Jpn. J. Appl. Phys.*, Vol. 20, pp. 243–247.
- [4]. Fearn R. M., Mullin T., Cliffe K. A., (1990), "Nonlinear flow phenomena in a symmetric sudden expansion", *J. Fluid Mechanics*, Vol. 211, pp. 595–608.
- [5]. Durst F., Pereira J. C. F., Cliffe K. A., (1993), "The plane symmetric sudden expansion flow at low Reynolds number", *J. Fluid Mechanics*, Vol. 248, pp. 567.
- [6]. Battaglia F., Tavener S. J., Kulkarni A. K., Merkle C. L., (1997), "Bifurcation of low Reynolds number flows in symmetric channels", *J. AIAA*, Vol. 35, pp. 99–105.
- [7]. Allerborn N., Nandakumar K., Raszillier H., Durst F., (1997), "Further contributions on the two-dimensional flow in a sudden expansion", *J. Fluid Mechanics*, Vol. 330, pp. 169.
- [8]. Revuelta A., (2005), "On the two-dimensional flow in a sudden expansion with large expansion ratios", *Phys. Fluids* Vol. 17, No. 028102.
- [9]. Abbott D. E., Kline S.J., (1962), "Experimental investigation of subsonic turbulent flow over single and double backward facing steps", *J. Basic Eng. Trans. ASME*, Vol. 84, No. 317.
- [10]. Mizushima J., Shiotani Y., (2000), "Structural instability of the bifurcation diagram for two-dimensional flow in a channel with a sudden expansion", *J. Fluid Mechanics*, Vol. 420, No. 131.
- [11]. Paulo J. Oliveira, (2003), "Asymmetric flows of viscoelastic fluids in symmetric planar expansion geometries", *J. Non-Newtonian Fluid Mech.* Vol. 114, pp. 33–63.
- [12]. Ternik P., Marn J., Zunic Z., (2006), "Non-Newtonian fluid flow through a planar symmetric expansion: shear-thickening fluids", *J. Non-Newtonian Fluid Mechanics*, Vol. 135, pp. 136–148.
- [13]. Drikakis D., (1997), "Bifurcation phenomena in incompressible sudden expansion flows", *J. Phys. Fluids*, Vol. 9, pp. 76–86.
- [14]. Hawa T., Rusak Z., (2001), "The dynamics of a laminar flow in a symmetric channel with a sudden expansion", *J. Fluid Mechanics*, Vol. 436, pp. 283–320.
- [15]. Mishra S., Jayaraman K., (2002), "Asymmetric flows in planar symmetric channels with large expansion ratio", *Int. J. Numer. Methods Fluids*, Vol. 38, pp. 945–962.
- [16]. Dagtekin I., Unsal M., (2011), "Numerical analysis of axisymmetric and planar sudden expansion flows for laminar regime". *Int J Numer Meth Fluids* 65: 1133–1144.
- [17]. Scott P.S., Mirza F.A., (1986), "A finite element analysis of laminar flows through planar and axisymmetric abrupt expansions". *Computers & Fluids* 14(4): 423–432.
- [18]. Oliveira P.J., Pinho F.T., Schulte A., (1998), "A general correlation for the local loss coefficient in Newtonian axisymmetric sudden expansions". *Int J of Heat and Fluid Flow* 19: 655–660.
- [19]. Schreck E., Schafer M., (2000), "Numerical study of bifurcation in three-dimensional sudden channel expansions". *Comput. Fluids* 29(583).
- [20]. Shapira M., Degani D., Weihs D., (1990), "Stability and existence of multiple solutions for viscous flow in suddenly enlarged channels". *Comp. Fluids* 18: 239–258.
- [21]. Durst F., Pereira J. C. F., Tropea C., (1993), "The plane symmetric sudden expansion flow at low Reynolds numbers". *J. Fluid Mech* 248(567).
- [22]. Fletcher D. F., Maskell S. J., Patrick M. A., (1985), "Heat and mass transfer computations for laminar flow in an axisymmetric sudden expansion". *Comp Fluids* 13: 207–221.
- [23]. Pinho F. T., Oliveira P. J., Miranda J. P., (2003), "Pressure losses in the laminar flow of shear-thinning power-law fluids across a sudden axisymmetric expansion". *Int J of Heat and Fluid Flow* 24: 747–761.
- [24]. Hawa T., Rusak Z., (2000), "Viscous flow in a slight axisymmetric channel with a sudden expansion". *Phys Fluids* 12: 22–57.
- [25]. Bell B. C., Surana K. S., (1994), "p-Version least squares finite element formulation for two-dimensional incompressible non-Newtonian isothermal and nonisothermal fluid flow". *Int J Numer Methods Fluids* 18: 127–162.
- [26]. Ternik P., (2009), "Planar sudden symmetric expansion flows and bifurcation phenomena of purely viscous shear-thinning fluids", *J. Non-Newtonian Fluid Mech.* Vol. 157, pp. 15–25.
- [27]. Manica R., De Bortoli A. L., (2004), "Simulation of sudden expansion flows for power-law fluids", *J. Non-Newtonian Fluid Mech.* Vol. 121, pp. 35–40.
- [28]. Neofytou P., (2006), "Transition to asymmetry of generalised Newtonian fluid flows through a symmetric sudden expansion", *J. Non-Newtonian Fluid Mech.* Vol. 133 pp. 132–140.
- [29]. Ternik P., Marn J., Zuni Z., (2006), "Non-Newtonian fluid flow through a planar symmetric expansion: Shear-thickening fluids", *J. Non-Newtonian Fluid Mech.* Vol. 135, pp. 136–148.
- [30]. Pak B., Cho Y. I., and Choi S. U. S., (1990), "Separation and reattachment of nonnewtonian fluid flows in a sudden expansion pipe", *Journal of Non-Newtonian Fluid Mechanics*, Vol. 37, pp. 175–199.

- [31]. M. Norouzi, M. M. Shahmardan, A. S. Zahiri, Bifurcation phenomena of inertial viscoelastic fluid flow through gradual expansions, *Journal of Rheology Acta*, Vol. 54, No. 123, pp. 423-435, 2015.
- [32]. Cruz, D. A., P. M. Coelho, and M. A. Alves. "A simplified method for calculating heat transfer coefficients and friction factors in laminar pipe flow of non-Newtonian fluids." *Journal of Heat Transfer* 134.9 (2012): 091703.
- [33]. Jalali, A., et al. "Numerical simulation of 3D viscoelastic developing flow and heat transfer in a rectangular duct with a nonlinear constitutive equation." *Korea-Australia Rheology Journal* 25.2 (2013): 95-105.
- [34]. Baptista, A., M. A. Alves, and P. M. Coelho. "Heat transfer in fully developed laminar flow of power law fluids." *Journal of Heat Transfer* 136.4 (2014): 041702.
- [35]. Alves, M. A., A. Baptista, and P. M. Coelho. "Simplified method for estimating heat transfer coefficients: constant wall temperature case." *Heat and Mass Transfer* 51.7 (2015): 1041-1047.
- [36]. Norouzi, M. "Analytical solution for the convection of Phan-Thien-Tanner fluids in isothermal pipes." *International Journal of Thermal Sciences* 108 (2016): 165-173.
- [37]. Letelier, Mario F., Cristian B. Hinojosa, and Dennis A. Siginer. "Analytical solution of the Graetz problem for non-linear viscoelastic fluids in tubes of arbitrary cross-section." *International Journal of Thermal Sciences* 111 (2017): 369-378.
- [38]. Shahbani-Zahiri, A., et al. "Numerical simulation of inertial flow of heated and cooled viscoelastic fluids inside a planar sudden expansion channel: investigation of stresses effects on the total dissipation." *Meccanica* 53.11-12 (2018): 2897-2920.

Amir haghightakhah, et. al. "Numerical investigation of non-Newtonian fluid flow in channels with local expansion." *IOSR Journal of Mechanical and Civil Engineering (IOSR-JMCE)*, 17(6), 2020, pp. 11-21.